Geochemical Perspectives Letters

Metamorphic evolution of carbonate-hosted microbial biosignatures

C.R. Cousins[1*], S. Mikhail[1,2], F. Foucher[3], A. Steele[2], F. Westall[3]

OPEN ACCESS

doi: 10.7185/geochemlet.2002

Abstract

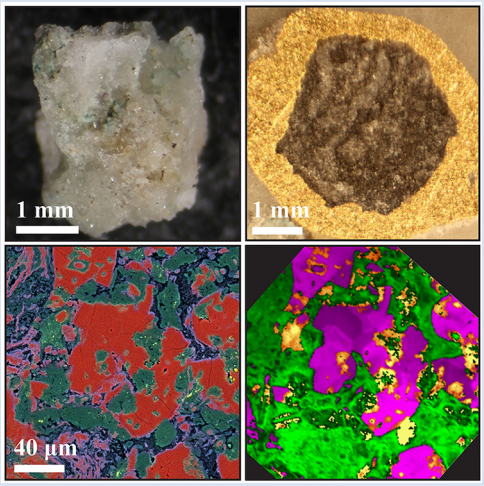

Microbial biosignature assemblages captured within mineral substrates experience extreme pressures (P) and temperatures (T) during rock burial and metamorphism. We subjected natural microbial biofilms hosted within thermal spring carbonate to six high pressure, high temperature (HPHT) conditions spanning 500 and 800 MPa and 200 to 550 °C, to investigate the initial petrographic transformation of organic and inorganic phases. We find biogenic and amorphous silica mineralises increasingly mature organic matter (OM) as temperature and pressure increase, with OM expelled from recrystallised calcite at the highest HPHT, captured within a quartz phase. Sulfur globules associated with microbial filaments persist across all HPHT conditions in association with microbially-derived kerogen. These data demonstrate how microbial material captured within chemically-precipitated sediments petrographically evolves in high grade rocks during their first stages of transformation.

Received 12 August 2019 | Accepted 6 December 2019 | Published 16 January 2020

Introduction

Our knowledge of microbiological evolution is informed by organic, morphological, and geochemical biosignatures preserved within a rock record that is destroyed or modified over geological time (Westall, 2008). Chemically-precipitated sediments, particularly carbonate and silica, host microfossils spanning much of Earth history, including in association with early evidence for microbial life on Earth (Moreau and Sharp, 2004; Westall, 2008; Wacey *et al.*, 2011; Djokic *et al.*, 2017). The petrographic relationships between microbially-derived kerogen and the inorganic matrix are important in establishing microfossil biogenicity (Brasier *et al.*, 2005; Wacey *et al.*, 2011; Foucher and Westall, 2013), in addition to understanding broader interations of microbe-mineral systems back into the early Archean (Westall *et al.*, 2015).

Significant experimental effort has furthered our understanding of microbial biomineralisation (Westall *et al.*, 1995; Orange *et al.*, 2012, 2014; Li *et al.*, 2013a and references therein; Gaboyer *et al.*, 2017). High pressure, high temperature (HPHT) experiments are now shedding light on microfossil taphonomy during geological sequestration, with a focus on thermal degradation of biogenic minerals (Li *et al.*, 2013b) and biomineralised cells (Li *et al.*, 2014). Experiments have demonstrated the persistence of microbiological structures such as iron oxide organominerals up to 250 °C and 140 MPa (Picard *et al.*, 2015a), and the preservation of lipids and polysaccharides within Fe-encrusted microbial cells at the same PT conditions (Picard *et al.*, 2015b). Recently, Alleon *et al.* (2016) showed that microbial entombment within silica limited the degradation of molecular biosignatures exposed to 25 MPa and 250 °C for 100 days.

As improving analytical techniques expand biosignature studies into increasingly metamorphosed terrains (Bernard *et al.*, 2007, 2010; Galvez *et al.*, 2012; Papineau *et al.*, 2019), there is a need to understand the influence of higher PT regimes (Li *et al.*, 2013a). We present an experimental investigation into the effects of HPHT on carbonate-hosted microbial biofilms from a natural thermal spring environment. We trace the first stages of petrographic evolution of geochemical and morphological sample components in response to 500 and 800 MPa and temperatures spanning 200 to 550 °C, significantly expanding the PT space previously investigated (Fig. 1a).

1. School of Earth and Environmental Sciences, University of St. Andrews, Irvine Building, North Street, St. Andrews, Fife, UK
2. Geophysical Laboratory, Carnegie Institute of Washington, Broad Branch Road, Washington D.C., USA
3. CNRS, Centre de Biophysique Moléculaire, UPR 4301, Rue Charles Sadron, CS80054, 45071 Orléans Cedex 2, France
* Corresponding author (email: crc9@st-andrews.ac.uk)

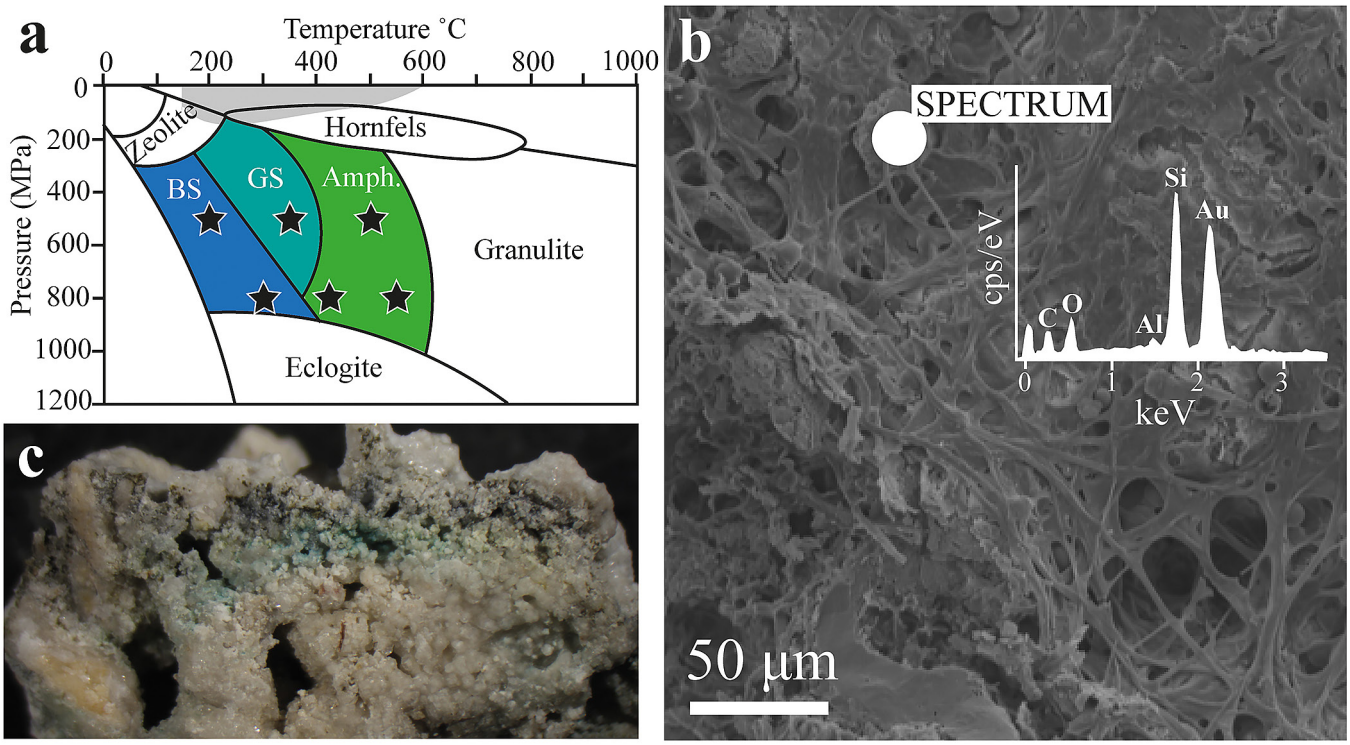

Figure 1 Starting material for experiments showing **(a)** Six high pressure, high temperature (HPHT) experimental conditions investigated and their corresponding metamorphic grades spanning lower and upper blueschist (BS), greenschist (GS) and amphibolite (Amph.). Grey depicts HPHT conditions investigated previously (Schiffbauer *et al.*, 2012; Li *et al.*, 2013b, 2014; Picard *et al.*, 2015a,b; Alleon *et al.*, 2016, 2017; Miot *et al.*, 2017). **(b)** Si-rich microbial filamentous material and coccoidal cell structures are observed under SEM in the the starting material, shown in **(c)** by a view ~ 1 cm across; forming Si-rich biofilms around calcite grains (Fig. S-1a,b).

Sample Material

Porous carbonate precipitates containing green, orange, and grey chasmolithic microbial communities (Fig. 1c) were collected from a CO_2 thermal spring (Jotun Spring; Banks *et al.*, 1998) in Spitzbergen, Svalbard, during the Arctic Mars Analog Svalbard Expeditions from 2006-2011 (Starke *et al.*, 2013). An air dried sample was subsampled into multiple ~2 mm^3 fragments for six HPHT experiments. Four additional fragments of this starting material were subjected to the same preparation and analytical techniques. Methods are described in the Supplementary Information.

Results

Visible light microscopy of polished HPHT samples reveal dark carbonised organic matter (OM) forming a compositional fabric within the calcite matrix, absent in the starting material (Fig. S-1a,c,d). Secondary electron imaging of a duplicate, acid etched 500 MPa, 350 °C sample shows mineralised biomass maintains its intact extracellular filamentous structure (Figs. 1b and S-1e) and coccoidal cell morphologies (Fig. S-1f). Intact diatom frustules are preserved at the lower PT conditions (500 MPa, 200 °C and 500 MPa, 350 °C), becoming structurally disintegrated in the higher PT experiments (500 MPa, 500 °C; 800 MPa, 300 °C and 800 MPa, 425 °C; Fig. S-1g,h).

Raman spectra of experimental sample surfaces exhibit peaks for carbonate (1100 cm^{-1}), and D1 (1360 cm^{-1}) and G (1610 cm^{-1}) carbon bands (Fig. 2; Pimenta *et al.*, 2007). An additional quartz band at 465 cm^{-1} is observed for the three highest temperature samples (425, 500, and 550 °C), irrespective of pressure. Secondary electron imaging shows OM transitioning from amorphous biogenic material with cellular structures in the starting material to increasingly crystalline structures as PT increases (Fig. 2). This is reflected in the changing carbon G-band centre and width, whereby temperatures of 350 °C and above produce a sharpened (more crystalline) G-band, and the increase in temperature from 200 to 550 °C also produces a peak centre shift to longer wavenumbers (Fig. S-2). Across all HPHT conditions OM maintains its original petrographic texture, either within a biofilm structure (Fig. 1c), or bound within diatom frustules (Fig. 1).

Raman spectroscopy and SEM+EDS elemental mapping of experimental sample surfaces show kerogenous material (D1 and G Raman bands) remains spatially-concurrent with the siliceous phase (Fig. 3). At the lowest PT condition (500 MPa, 200 °C), petrographic textures are largely indistinguishable from those in the starting material. At 800 MPa, 425 °C (Fig. 3d) these phases form compositional fabrics, where the organic-rich phase exists within silicified or quartz-rich fabrics, which also have elevated Fe (Fig. 4h,i). With increasing PT, the silica-organic phase becomes partitioned from the recrystallising calcite, eventually forming discrete petrographic end members at 800 MPa and 550 °C, whereby kerogen either forms an organic carbonaceous film around quartz crystals (Fig. 3e) or is captured within the quartz itself (Fig. 3f). Water degassing is observed in the carbonate matrix for samples treated at 500 MPa, 350 °C; 500 MPa, 500 °C and 800 MPa, 425 °C (Fig. S-4b,c,e), and extensive fracturing (Fig. S-4b,c,d) is observed at 500 MPa (350 °C and 500 °C) and 800 MPa (300 °C).

Finally, discrete clusters of sulfur globules 1 – 3 µm in size are observed within the starting material (Fig. 4a,b). These globules persist through all thermal conditions at 800 MPa, and at 500 MPa, 500 °C, remaining petrographically associated with the siliceous kerogen-bearing phase (Fig. 4a-g). At the highest PT condition (800 MPa, 550 °C), globules become irregular structures (Fig. 4f). Fe co-occurs within the Si phase

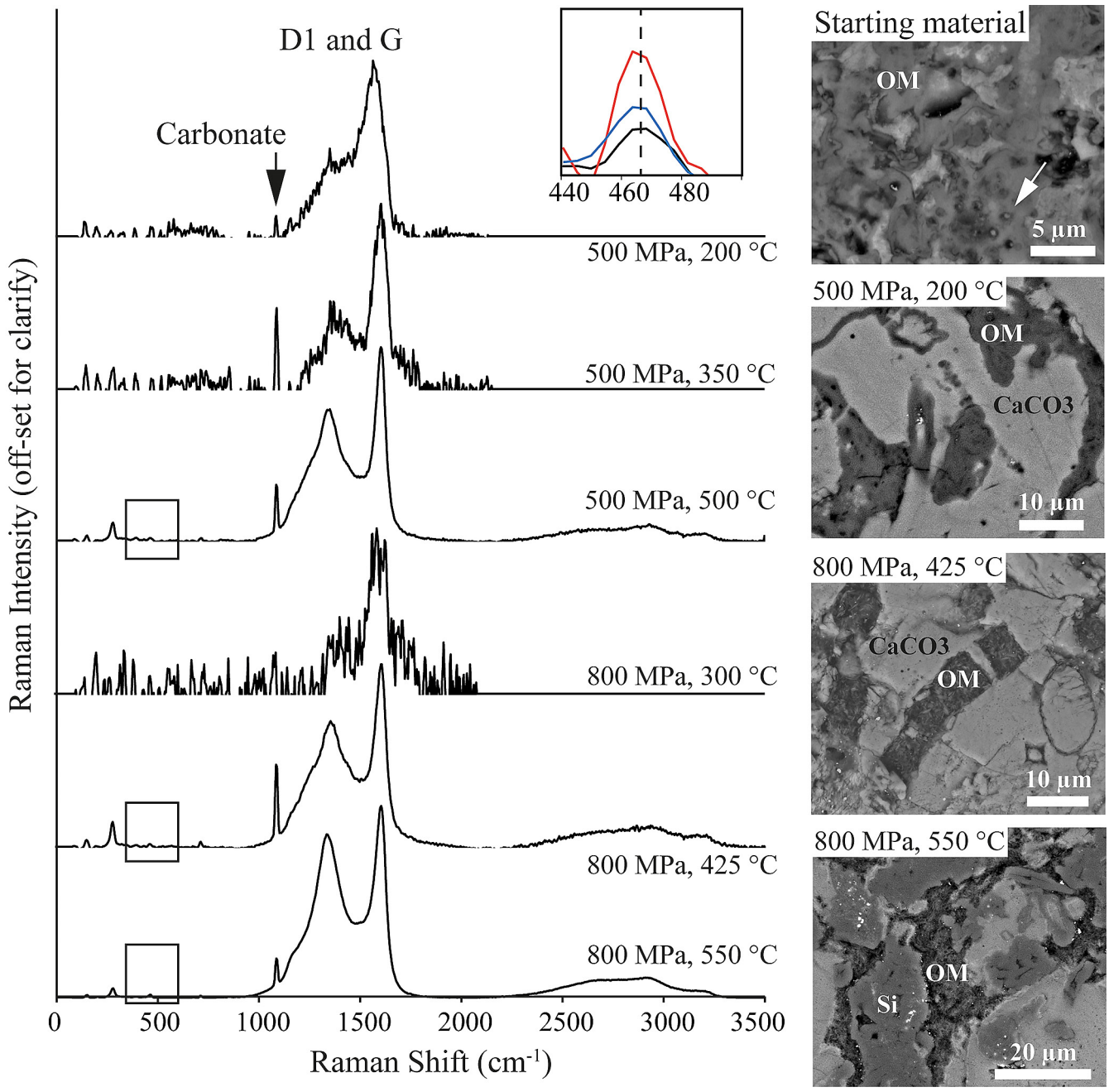

Figure 2 Evolution of D1 (~1360 cm^{-1}) and G (~1610 cm^{-1}) Raman peaks from experimental samples, and the increasing 467 cm^{-1} quartz peak at 425, 500, and 550 °C (box inset); and corresponding SEM images showing the textural evolution of OM mineralisation within the carbonate ($CaCO_3$) matrix and siliceous (Si) phases Individual cells in the amorphous organic matrix can be seen in the starting material (arrows). Unprocessed Raman spectra are given in Figure S-3.

for all samples, including in association with the S globules (Fig. 4h). Despite being a strong Raman scatterer, elemental sulfur was not detected by Raman spectroscopy (Fig. 2).

Discussion

Within the bounds of a closed system, mm- to micron-scale elemental (Si, S, Fe) biosignatures and microbially-derived kerogen maintain their petrographic relationship throughout initial exposure to HPHT (Fig. S-1c). *In situ* silicification of biomass occurs without petrographic disruption to the captured OM. With increasing PT, the organic-rich amorphous siliceous phase crystallises into α-quartz, and the originally porous calcite anneals into a crystalline matrix at 800 MPa, 550 °C, expelling siliceous OM-bearing material. Extensive fracturing of the carbonate matrix observed at 800 MPa, 300 °C may be detrimental to preservation of biosignatures in comparison to an annealed calcite matrix, as the fractures would provide pathways for altering fluids. Disintegration of diatom frustules may be an additional source of Si as PT conditions increase.

Displacement of kerogen during diagenetic coarsening of quartz has been identified as a mechanism to explain petrographic relationships in the microfossil-bearing Gunflint chert (Moreau and Sharp, 2004; Foucher and Westall, 2013). This has implications for the longevity of biosignatures, whereby the quartz fraction resists weathering or secondary aqueous alteration, protecting captured OM (Toporski *et al.*, 2002). The preservation of OM within silicious material is consistent with Alleon *et al.* (2016), who demonstrated the role of silica in limiting thermally-induced molecular degradation of OM in experimental samples. The transformation of Fe minerals to more stable, crystalline phases has also been shown to be conducive to the preservation of organic components (Ferris

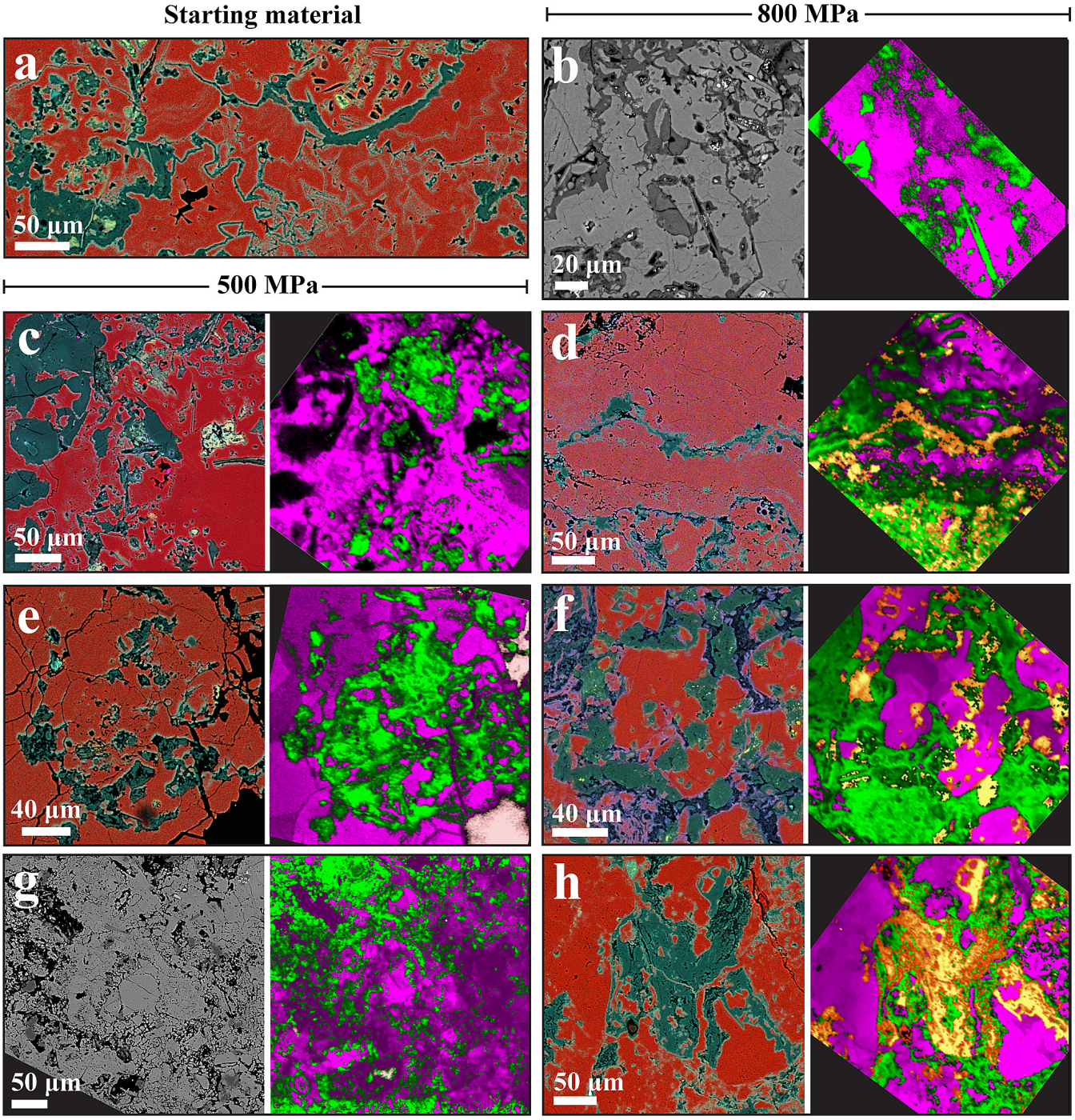

Figure 3 BSE+EDS elemental maps or plain BSE image (left), where red = Ca and green = Si, and corresponding Raman maps (right) of the same region, where fuchsia = calcite (1006 cm^{-1} band), orange/yellow = quartz (465 cm^{-1} band), green = carbon (combined D1 and G bands), light pink = resin, black = masked fluorescence. **(a)** Starting material; **(b)** 800 MPa, 300 °C; **(c)** 500 MPa, 200 °C; **(d)** 800 MPa, 425 °C; **(e)** 500 MPa, 350 °C; **(f)** 800 MPa, 550 °C; **(g)** 500 MPa, 500 °C; **(h)** 800 MPa, 550 °C. EDS spectra are provided in Figure S-5.

et al., 1988; Picard *et al.*, 2015a). Finally, the sulfur globules observed in the starting material and experimental samples are consistent in size and shape to intracellular sulfur globules found within filamentous sulfide oxidising bacteria (Dahl and Prange, 2006). Their preservation at the highest HPHT condition holds promise for establishing the biogenicity of similar features in filmentous microfossils (Wacey *et al.*, 2011; Bailey *et al.*, 2013) and distinguishing them from abiotic S microstructures (Cosmidis and Templeton, 2016).

While the OM Raman spectra are relatively close to those observed in the Gunflint and Draken formation (Foucher *et al.*, 2015), such experiments are inheritently limited by their short duration. Even with the addition of P, Raman D1 and G bands of experiment sample OM are broader than those from metasediments of equivalent metamorphic grade (Beyssac *et al.*, 2002), indicating they are less mature. This limitation was also observed by Li *et al.* (2014) for experiments at similar temperatures (300 °C, 600 °C) in the absence of pressure.

Conclusions

This study presents an experimental investigation into the first stages of HPHT evolution of microbial biosignatures within a natural siliceous-carbonate matrix. While thermal maturation of OM is well understood (Vandenbroucke and

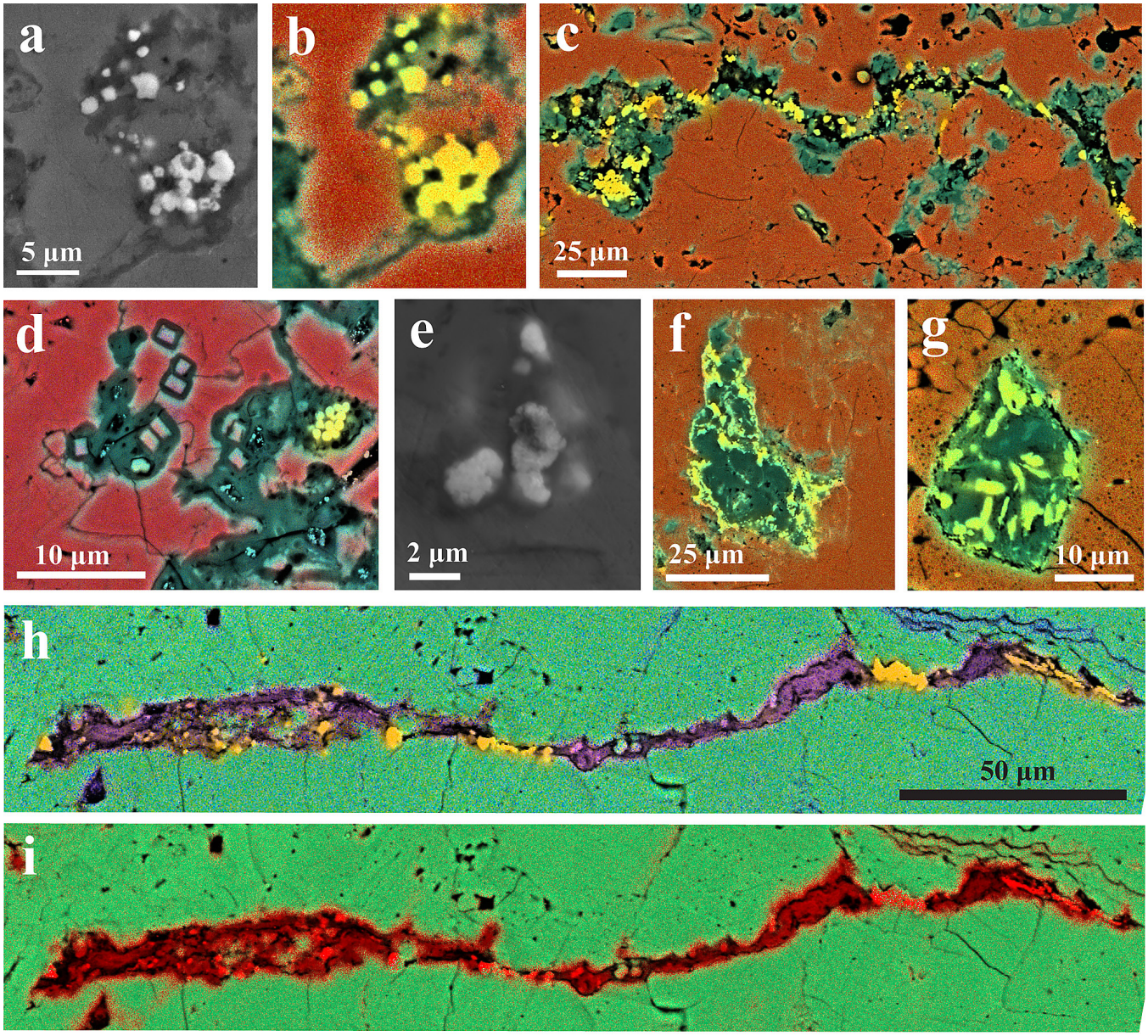

Figure 4 **(a – g)** BSE+EDS elemental maps (red = Ca, green = Si, yellow = S) and SEM images of sulfur globules in **(a, b)** Starting material; **(c)** 800 MPa, 425 °C; **(d, e)** 800 MPa, 300 °C; **(f)** 800 MPa, 550 °C; and **(g)** 500 MPa, 500 °C; **(h)** BSE+EDS elemental map showing the co-location of Fe (Fe = purple) with S (S = yellow) within a silica-rich (Si = red) fabric **(i)** in the 800 MPa, 425 °C experiment.

Largeau, 2007), we show that the early effects of temperature and pressure play an important role in the petrographic redistribution and capture of OM due to the transformation of the low temperature silica and carbonate phases. We demonstrate that exposure up to 800 MPa and 550 °C does not disrupt the petrographic relationship of captured microbial material with its inorganic host phase during the first stages of metamorphism. Future experimental work should address open system effects, including the influence of fluids on the modification of sample components, and longer duration experiments.

Acknowledgements

This work was funded by a Royal Society of Edinburgh Research Fellowship. FF and FW acknowledge funding from the CNRS and CNES.

Editor: Karim Benzerara

Additional Information

Supplementary Information accompanies this letter at http://www.geochemicalperspectivesletters.org/article2002.

Cite this letter as: Cousins, C., Mikhail, S., Foucher, F., Steele, A., Westall, F. (2020) Metamorphic evolution of carbonate-hosted microbial biosignatures. *Geochem. Persp. Let.* 12, 40-45.

References

Alleon, J., Bernard, S., Le Guillou, C., Daval, D., Skouri-Panet, F., Pont, S., Delbes, L., Robert, F. (2016) Early entombment within silica minimizes the molecular degradation of microorganisms during advanced diagenesis. *Chemical Geology* 437, 98-108.

Alleon, J., Bernard, S., Le Guillou, C., Daval, D., Skouri-Panet, F., Kuga, M., Robert, F. (2017) Organic molecular heterogeneities can withstand diagenesis. *Scientific Reports* 7, 1508.

Bailey, J.V., Corsetti, F.A., Greene, S.E., Crosby, C.H., Liu, P., Orphan, V.J. (2013) Filamentous sulfur bacteria preserved in modern and ancient phosphatic sediments: implications for the role of oxygen and bacteria in phosphogenesis. *Geobiology* 11, 397-405.

Banks, D., Sletten, R.S., Haldorsen, S., Dale, B., Heim, M., Swensen, B. (1998) The Thermal Springs of Bockfjord, Svalbard: Occurrence and Major Ion Hydrochemistry. *Geothermics* 27, 445-467.

Bernard, S., Benzerara, K., Beyssac, O., Mgnguy, N., Guyot, F., Brown Jr., G.E., Goffe, B. (2007) Exceptional preservation of fossil plant spores in high-pressure metamorphic rocks. *Earth and Planetary Science Letters* 262, 257-272

Bernard, S., Benzerara, K., Beyssac, O., Brown, G.E. (2010) Multiscale characterization of pyritized plant tissues in blueschist facies metamorphic rocks. *Geochimica Cosmochimica Acta* 74, 5054-5068.

Beyssac, O., Goffé, B, Chopin, C., Rouzaud, J.N. (2002) Raman spectra of carbonaceous material in metasediments: a new geothermometer. *Journal of Metamorphic et Geology* 20, 859-871.

Brasier, M.D., Green, O.R., Lindsay, J.F., McLoughlin, N., Steele, A., Stoakes, C. (2005) Critical testing of Earth's oldest putative fossil assemblage from the ~3.5 Ga Apex chert, Chinaman Creek, Western Australia. *Precambrian Research* 140, 55-102.

Cosmidis, J., Templeton, A.S. (2016) Self-assembly of biomorphic carbon/sulfur microstructures in sulfidic environments. *Nature Communications* 7, 12812.

Dahl, C., Prange, A. (2006) Bacterial Sulfur Globules: Occurrence, Structure and Metabolism. In: Shively J.M. (Eds) *Inclusions in Prokaryotes*. Springer, Berlin, Heidelberg, 21-51.

Djokic, T., Van Kranendonk, M., Campbell, K.A., Walter, M.R., Ward, C.R. (2017) Earliest signs of life on land preserved in ca. 3.5 Ga hot spring deposits. *Nature Communications* 8, 15263, doi: 10.1038/ncomms15263.

Ferris, F.G., Fyfe, W.S., Beveridge, T.J. (1988) Metallic ion binding by *Bacillus subtilis*: implications for the fossilization of microorganisms. *Geology* 16, 153-157.

Foucher, F., Westall, F. (2013) Raman Imaging of Metastable Opal in Carbonaceous Microfossils of the 700–800 Ma Old Draken Formation. *Astrobiology* 13, 57-67.

Foucher, F., Ammar, M.R., Westall, F. (2015) Revealing the biotic origin of silicified Precambrian carbonaceous microstructures using Raman spectroscopic mapping, a potential method for the detection of microfossils on Mars. *Journal of Raman Spectroscopy* 46, 873-879.

Gaboyer, F., Milbeau, C.L., Bohmeier, M., Schwendner, P., Vannier, P., Beblo-Vranesevic, K., Rabbow, E., Foucher, F., Gautret, P., Guégan, R., Richard, A., Sauldubois, A., Richmann, P., Perras, A.K., Moissl-Eichinger, C., Cockell, C.S., Rettberg, P., Marteinsson, V., Monaghan, E., Ehrenfreund, P., Garcia-Descalzo, L., Gomez, F., Malki, M., Amils, R., Cabezas, P., Walter, N., Westall, F. (2017) Mineralization and Preservation of an extremotolerant Bacterium Isolated from an Early Mars Analog Environment. *Scientific Reports* 7, 14.

Galvez, M.W., Beyssac, O., Benzerra, K., Bernard, S., Menguy, N., Cox, C.S., Martinez, I., Johnston, M.R., Brown Jr, G.E. (2012) Morphological preservation of carbonaceous plant fossils in blueschist metamorphic rocks from New Zealand. *Geobiology* 10, 118-129.

Li, J., Benzerara, K., Bernard, S., Beyssac, O. (2013a) The link between biomineralization and fossilization of bacteria: Insights from field and experimental studies. *Chemical Geology* 359, 49-69.

Li, Y.L., Konhauser, K.O., Kappler, A., Hao X.L. (2013b) Experimental low-grade alteration of biogenic magnetite indicates microbial involvement in generation of banded iron formations. *Earth and Planetary Science Letters*, 361, 229-237.

Li, J., Bernard, S., Benzerara, K., Beyssac, O., Allard, T., Cosmidis, J., Moussou, J. (2014) Impact of biomineralization on the preservation of microorganisms during fossilization: An experimental perspective. *Earth and Planetary Science Letters* 400, 113-122.

Moreau, J.W., Sharp, T.G. (2004) A Transmission Electron Microscopy Study of Silica and Kerogen Biosignatures in ~1.9 Ga Gunflint Microfossils. *Astrobiology* 4, 196-210.

Miot, J., Bernard, S., Bourreau, M., Guyot, F., Kish, A. (2017) Experimental maturation of Archaea encrusted by Fe-phosphates. *Scientific Reports* 7, 16984.

Orange, F., Disnar, J.R., Gautret, P., Westall, F., Bienvenu, N., Lottier, N., Prieur, D. (2012) Preservation and evolution of organic matter during experimental fossilisation of the hyperthermophilic archaea *Methanocaldococcus jannaschii*. *Origins of Life and Evolution of Biospheres* 42, 587-609.

Orange, F., Dupont, S., Goff, O.L., Bienvenu, N., Disnar, J.R., Westall, F., Le Romancer, M., (2014) Experimental fossilization of the thermophilic Gram-positive Bacterium Geobacillus SP7A: a long duration preservation study. *Geomicrobiology Journal* 31, 578-589.

Papineau, D., DeGregorio, B., Sagar, J., Thorogate, R., Wang, J., Nittler, L., Kilcoyne, D.A., Marbach, H., Drost, M. Thornton, G. (2019) Fossil biomass preserved as graphitic carbon in a late Paleoproterozoic banded iron formation metamorphosed at more than 550 °C. *Journal of the Geological Society of London* 176, 651-668.

Picard, A., Kappler, A., Schmid, G., Quaroni, L., Obst, M. (2015a) Experimental diagenesis of organo-mineral structures formed by microaerophilic Fe(II)-oxidizing bacteria. *Nature Communications* 6, 6277 (2015), doi: 10.1038/ncomms7277.

Picard, A., Obst, M., Schmid, G., Zeitvogel, F., Kappler, A. (2015b) Limited influence of Si on the preservation of Fe mineral-encrusted microbial cells during experimental diagenesis *Geobiology* 14, 276-292.

Pimenta, M.A., Dresselhaus, G., Dresselhaus, M.S., Cancado, L.G., Jorio, A., Saito, R. (2007) Studying disorder in graphite-based systems by Raman spectroscopy. *Physical Chemistry Chemical Physics* 9, 1276-1291.

Schiffbauer, J. D., Wallace, A.F., Hunter, J.L., Kowalewski, M., Bodnar, R.J., Xiao, S. (2012) Thermally-induced structural and chemical alteration of organic-walled microfossils: an experimental approach to understanding fossil preservation in metasediments. *Geobiology* 10, 402-423.

Starke, V., Kirshtein, J., Fogel, M.L., Steele, A. (2013) Microbial community composition and endolith colonization at an Arctic thermal spring are driven by calcite precipitation. *Environmental Microbiology Reports* 5, 648-659, doi: 10.1111/1758-2229.12063.

Toporski, J.K., Steele, A., Westall, F., Thomas-Keprta, K.L., McKay, D.S. (2002) The simulated silicification of bacteria - new clues to the modes and timing of bacterial preservation and implications for the search for extraterrestrial microfossils. *Astrobiology* 2, 1-26.

Wacey, D., Kilburn, M.R., Saunders, M., Cliff, J., Brasier, M.D. (2011) Microfossils of sulphur-metabolizing cells in 3.4-billion-year-old rocks of Western Australia. *Nature Geoscience* 4, 698-702.

Westall, F., Boni, L., Guerzoni, E. (1995) The experimental silicification of microorganisms. *Palaeontology* 38, 495-528.

Westall, F. (2008) Morphological Biosignatures in Early Terrestrial and Extraterrestrial Materials. *Space Science Reviews* 135, 95-114.

Westall, F., Campbell, K.A., Bréhéret, J.G., Foucher, F., Gautret, P., Hubert, A., Sorieul, S., Grassineau, N., Guido, D.M. (2015) Archean (3.33 Ga) microbe-sediment systems were diverse and flourished in a hydrothermal context. *Geology* 43, 615-618.

Geochemical Perspectives Letters

Metamorphic evolution of carbonate-hosted microbial biosignatures

C. Cousins, S. Mikhail, F. Foucher, A. Steele, F. Westall

Supplementary Information

The Supplementary Information includes:

- Methods
- Figures S-1 to S-5

Methods

Experimental HPHT conditions

Individual samples were exposed to HPHT conditions for 24 hours using a Depths of the Earth QUICKpress™ piston-cylinder press at the Geophysical Laboratory, Carnegie Institute of Washington, USA. For a review on experimental petrology, including an overview of the piston cylinder apparatus, see Holloway and Wood, (1988). The samples were sealed by welding in gold capsules. The assembly consisted of a barium carbonate outer sleeve wrapped in lead foil enveloping a pyrex sleeve containing the graphite furnace and crushable MgO components. The welded gold capsules were hosted within MgO sleeves and MgO powder was pressed into the spaces to ensure static pressure conditions. Note, while external pressure conditions applied were static, the heterogeneous nature of natural material mean that internally, uniform compaction during static compression cannot be expected, and is an important aspect of replicating natural systems. Temperature was measured using a type-S thermocouple and monitored and maintained using a Eurotherm control. Six HPHT conditions were selected based on their representation of metamorphic PT-space (Fig. S-1c). These were three experiments at 500 MPa: (i) 500 MPa, 200 °C; (ii) 500 MPa, 350 °C; (iii) 500 MPa, 500 °C; and three experiments at 800 MPa: (iv) 800 MPa, 300 °C; (v) 800 MPa, 425 °C; (vi) 800 MPa, 550 °C. Of these, an additional duplicate run of the 500 MPa, 350 °C experiment was conducted for additional analysis of an acid-etched, unpolished surface. Experiments ran for 24 hours, after which they were quenched by shutting off the power to the press while maintaining pressure until the sample reached room temperature. For subsequent analysis, each experimental charge and the positive controls were rough-polished on one side using alumina polishing powder to reveal a sample surface, before being mounted in epoxy resin and polished using alumina polishing powder. Polished starting material samples and experiment charges were first analysed by Raman spectroscopy, followed by SEM analysis. The duplicate 500 MPa, 350 °C experimental sample and an additional starting material sample were etched on the sample surface to remove a surface layer of carbonate, revealing organic and siliceous sample components for SEM imaging. Samples were etched with 10 % HCl for 30 minutes, rinsed in DI water, then air-dried. These samples were not polished so to preserve the natural structures revealed by the etching process.

Raman Spectroscopy

Polished samples were analysed using a WITec Alpha500 Confocal Raman spectrometer at CNRS, CBM, Orléans, France. For this, a

Nd:YAG frequency doubled green laser (wavelength 532 nm) was used. Initial transmitted light observation of the sample was performed and images of target areas captured. Maps were acquired using a Nikon E Plan 50x objective with a numerical aperture N.A. = 0.75. The corresponding diameter of the laser spot was thus approximately 850 nm (d=1.22*Lambda/N.A.). The grating used was a 600 g/mm associated with a spectral resolution of approximately 3.8 cm^{-1}. Raman imaging was conducted by scanning the samples over areas ranging from 80 x 80 μm^2 and 600 x 600 μm^2. Maps were acquired during continuous scans whereby the sample is continuously moved below the laser. The exposure time is thus dependent of the spot size, the scan size, the resolution of the map and the integration time (more details can be found in Foucher *et al*., 2017). Power was tuned in order to prevent burning of sample materials, which was determined by visual inspection before and after data acquisition. The collected imaging data were then analysed using Witec proprietary software (Witec Project). False-colour compositional maps were produced using the peak area over the baseline. For low P T samples, masks were created to select only pixels associated with satisfactory signal to noise ratio for the carbonaceous mateer (low background level and high G band intensity), and the corresponding spectra were averaged. For higher P T samples, the signal to noise was good enough to obtain the average spectrum from the full maps.

Field Emission Gun-Scanning Electron Microscope analysis

Following Raman spectral mapping, experimental and starting material samples were carbon coated and analysed using a Field Emission Gun Scanning Electron Microscope (FEG-SEM) at the University of Edinburgh, UK, with elemental quantification achieved via Energy Dispersive System (EDS) analysis. An accelerating voltage of 20 KeV and working distance of 7 mm was used.

Supplementary Figures

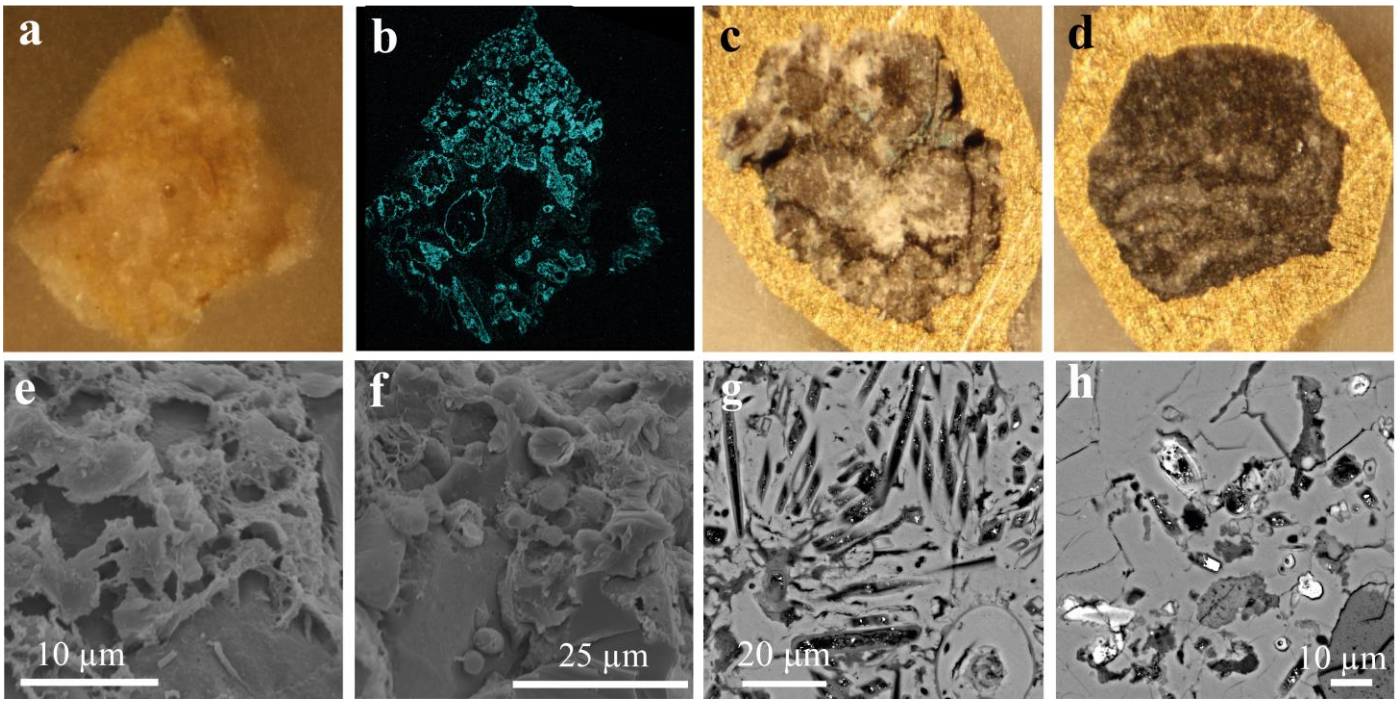

Figure S-1 Reflected light microscope images **(a, c, d)** of exposed polished surfaces (all approximately 2-3 mm across) of **(a)** starting material **(c)** 800 MPa, 300 °C experiment; and **(d)** 800 MPa, 425 °C experiment, where dark organic matter can be seen forming a defined fabric within the light grey calcite matrix, a feature absent from the starting material. **(b)** EDS elemental map of Si (cyan) of the exposed surface in (a); SEM images **(e-f)** of the acid-etched duplicate 500 MPa, 350 °C experiment showing **(e)** silicified filament structures and **(f)** intact coccoidal structures; and (g=h) SEM image showing intact **(g)** and partially-degraded **(h)** diatom frustule structures in the starting material and at 800 MPa, 300 °C, respectively.

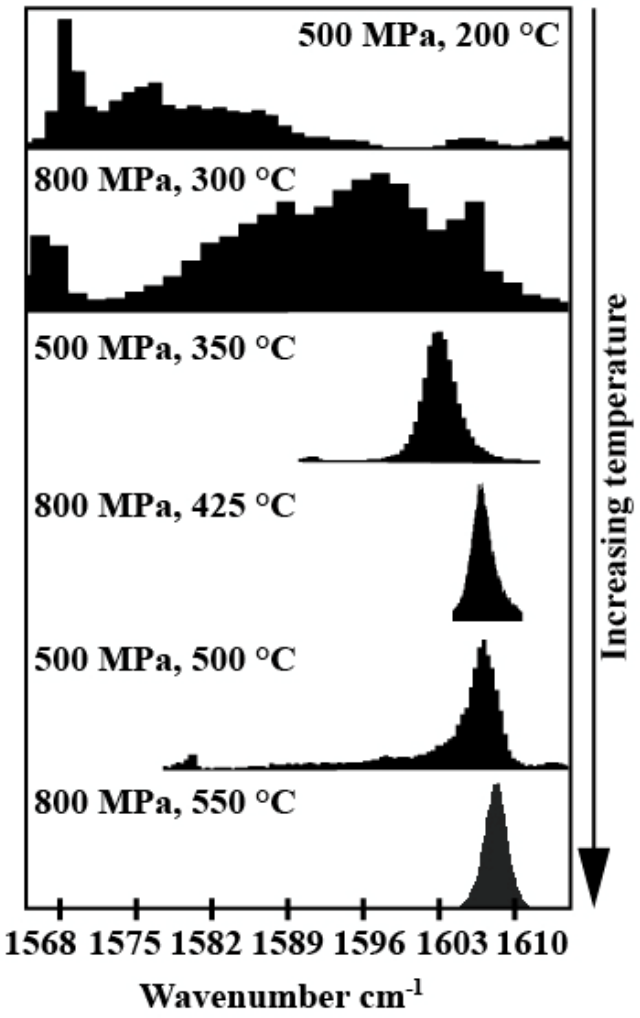

Figure S-2 Pixel histograms of the G band peak centre across the six experiments, in order of increasing temperature.

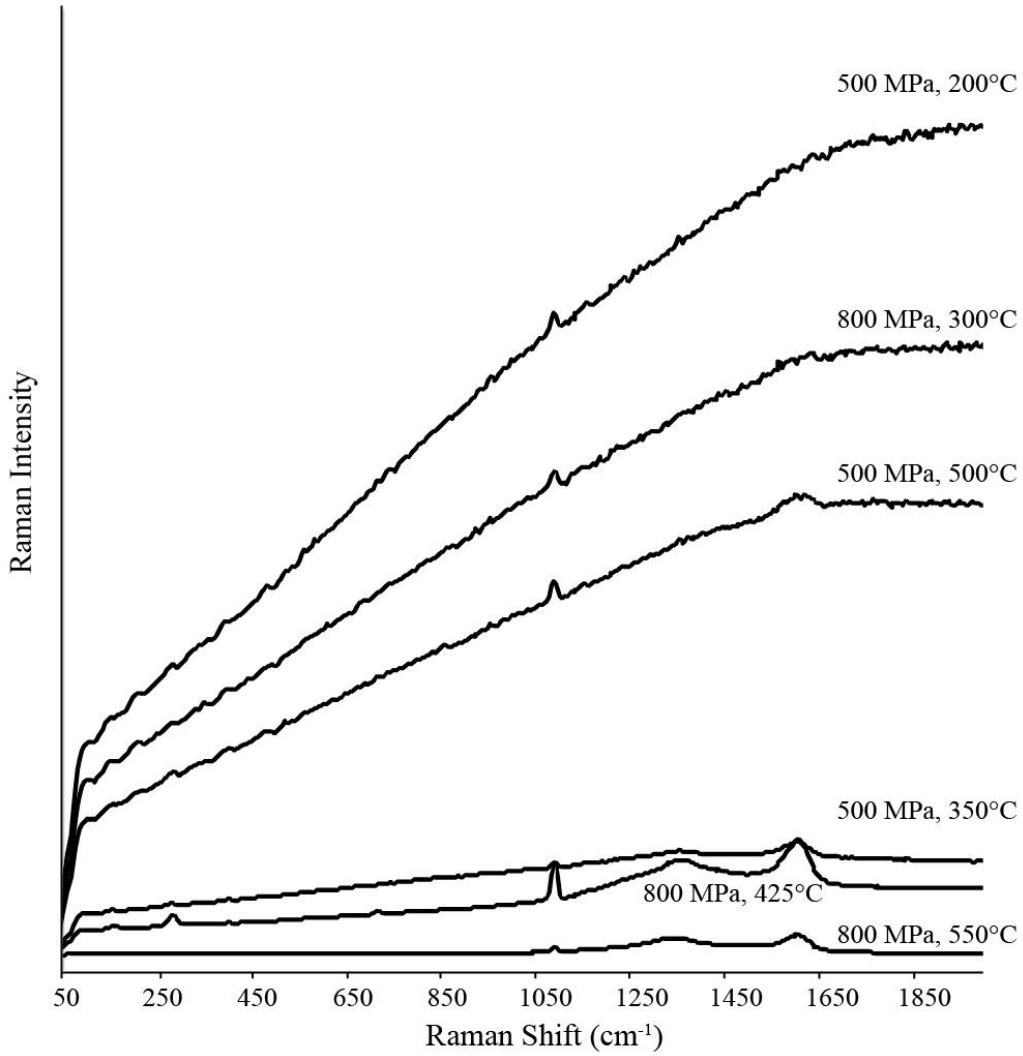

Figure S-3 Raman spectra for the six experimental conditions before background fluorescence is removed. Note that for the starting material, very high fluorescence masked all Raman signals, and so is not included here.

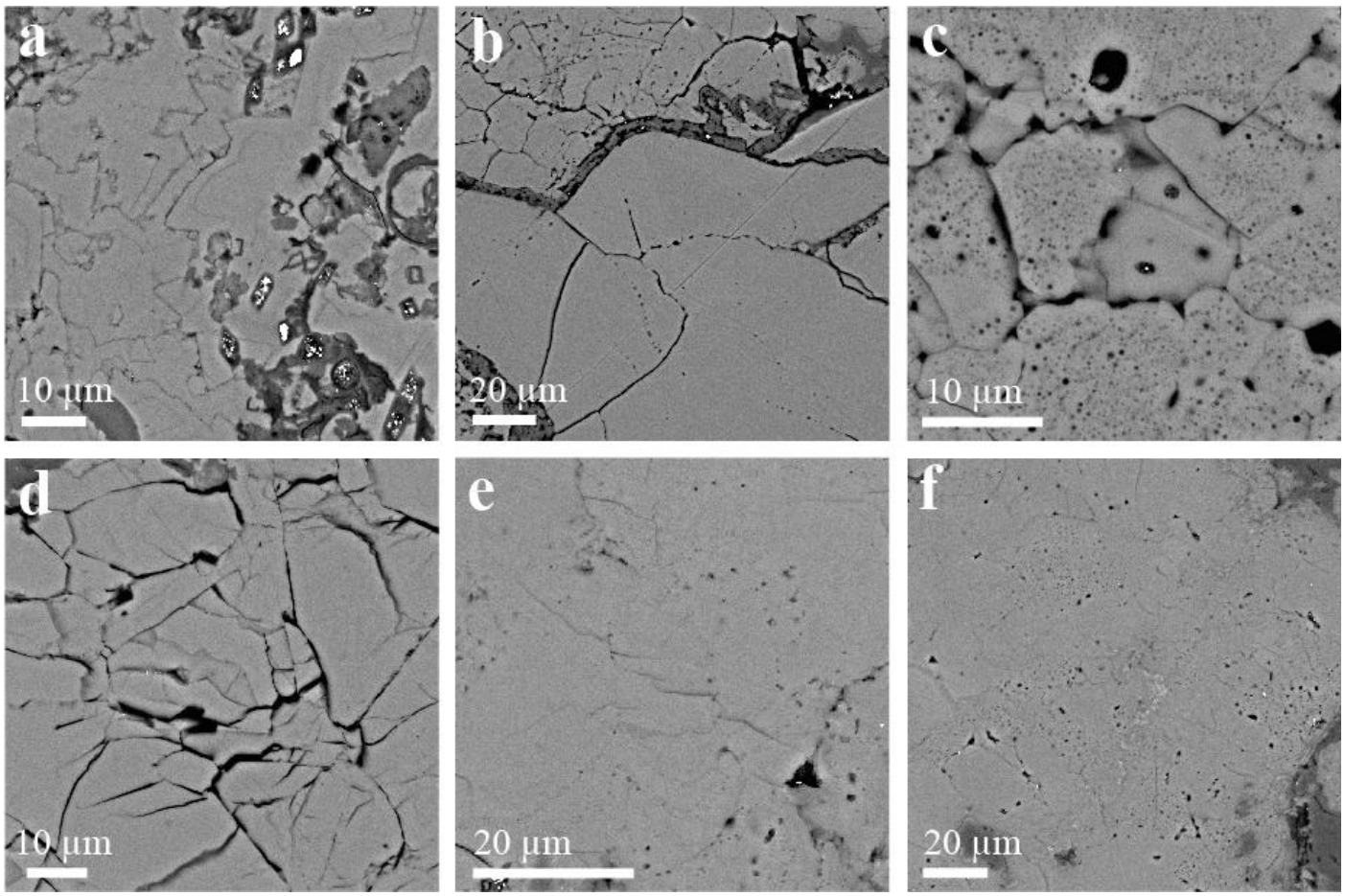

Figure S-4 SEM images of experimental samples showing **(a)** 500 MPa, 200 °C with no degassing or fracturing; **(b)** fracturing and minor degassing at 500 MPa, 350 °C; **(c)** fracturing and extensive degassing at 500 MPa, 500 °C; **(d)** fracturing but no degassing at 800 MPa, 300 °C, **(e)** 800 MPa, 425 °C with minor degassing and no fracturing; and **(f)** recrystallisation of the calcite matrix and minor degassing at 800 MPa, 550 °C.

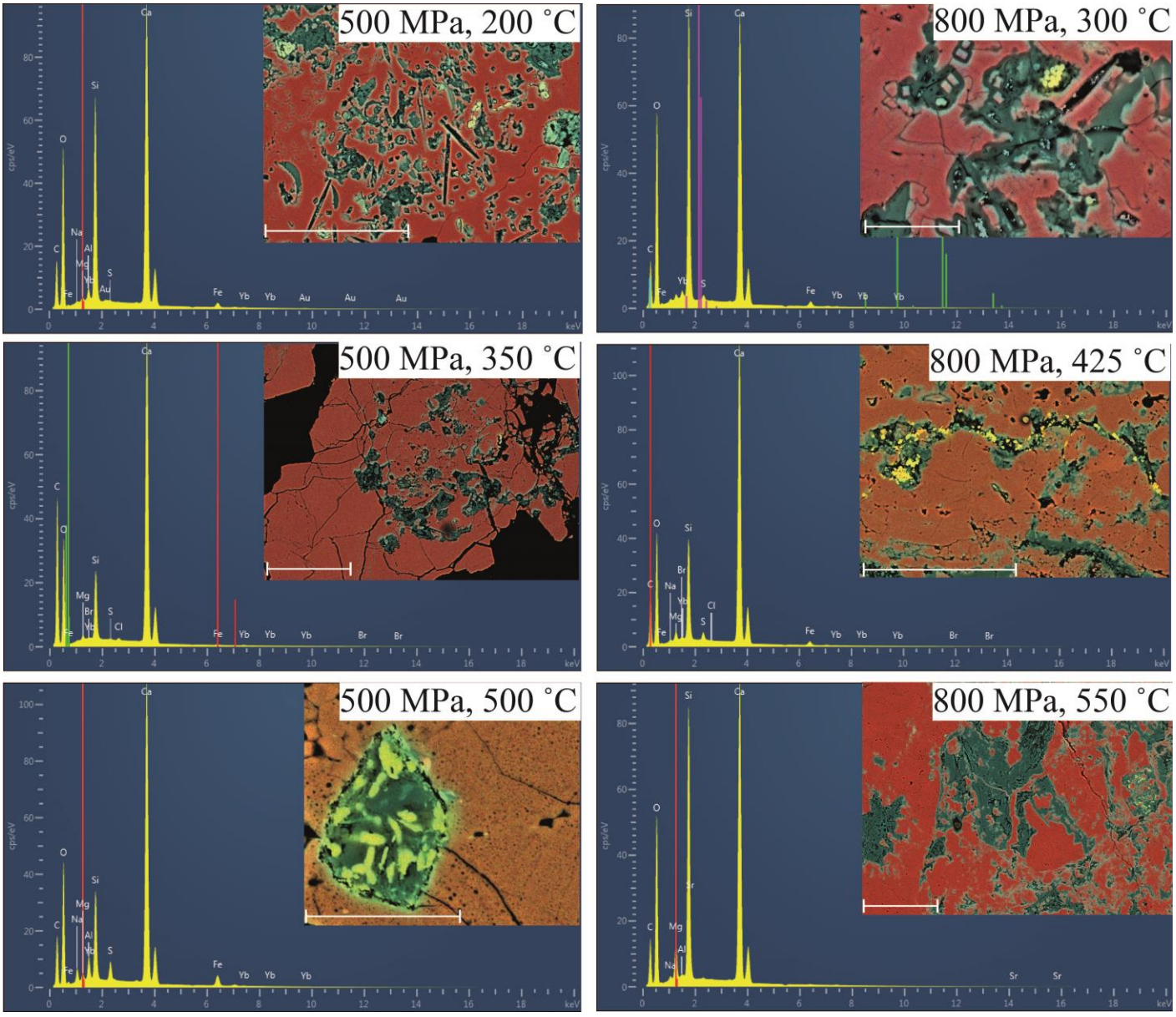

Figure S-5 EDS spectra measured from the example mapped regions depicted within the manuscript. Scale bar = 100 µm, with the exception of 500 MPa, 500 °C and 800 MPa, 300 °C, which are 25 µm.

Supplementary Information References

Foucher, F., Guimbretière, G., Borst, N., Westall, F. (2017) Petrographical and Mineralogical Applications of Raman Mapping. In: Maaz, K. (Ed.) *Raman Spectroscopy and Applications*. IntechOpen.

Holloway, J.R., Wood, B.J. (1988) Simulating the Earth: Experimental Geochemistry. Unwin Hyman Inc, London, pp. 1-196.